Numerical Methods in Civil Engineering

Seismic loss analysis of buckling-restrained braced frames considering the effects of modeling uncertainties

A. M. Azimi*, E. Khojastehfar**

ARTICLE INFO

Article history:
Received:
August 2018.
Revised:
November 2018.
Accepted:
December 2018.

Keywords:
Seismic loss analysis
BRBF
Modeling uncertainties
Expected annual loss
IDA

Abstract:

While the design criteria for buckling-restrained braced frames are advancing, understanding the functional behavior of these types of frames during the occuring earthquakes can considerably contribute in the evolution of the design criteria for these frames. In this regard, taking the modeling uncertainties into account will help in carrying out a more rational seismic performance assessment and seismic design of these types of structures. The main goal of this manuscript is to include the modeling uncertainties in the seismic loss mathematical curves of the buckling-restrained braced frames (BRBF). The variation of the modulus of elasticity and the yield strength constitute the sources of the uncertainties for this study. The two-dimensional 4-, 8-, and 12-story frames ,selected from symmetrical three-dimensional structures, were studied. Finally, it was concluded that the uncertainties existed in the yield stress and the modulus of elasticity parameters were more effective on the probabilistic seismic demand curves for the lower intensity levels, than the higher strong ground motion intensities. Besides all these, the variations of seismic-induced loss curves are presented considering the effect of the uncertainties compared to those neglecting the uncertainties. The calculated loss curves confirm the significance of taking the sources of uncertainties into account in the seismic loss analysis of the structures.

1. Introduction

In the conventional seismic design codes and standards, the effect of uncertainties on the applied actions and the capacity of structural members are taken into account by the load and resistance safety factors, respectively. Given the possible inaccuracies of this method for the earthquake effects due to large inherent uncertainties, the next generation of performance-based earthquake engineering codes was developed to directly include the sources of uncertainties in the assessment of the seismic performance of structures [1]. In this regard, the seismic performance-based assessment method proposed by the Pacific Earthquake Engineering Research Center (*PEER*) Institute tries to take different uncertainties into account by combining the probability curves of earthquake hazard, structural seismic response, fragility curves, and loss models.

** MSc Graduate, Vali-e-Asr University of Rafsanjan, Rafsanjan, Iran.*
*** Corresponding author: Assistant Professor, Vali-e-Asr University of Rafsanjan, Rafsanjan, Iran. Email: e.khojastehfar@vru.ac.ir*

Consequently, the seismic performance of structures is expressed by the seismic loss curve, in which the contributed uncertainties are included. Applying this consistent probabilistic framework, while different sources of uncertainties are involved, it helps with obtaining a more realistic final loss curve and making more rational decisions.

In general, uncertainty sources are classified into two main groups of ‘aleatory’ and ‘epistemic’. Kiureghian and Ditlevsen [2] introduced this general classification and studied their effects on the seismic risk, reliability analysis, performance-based design, and code-based design methods. The aleatory randomness is initiated by the inherent random nature of the physical quantities (such as the variability of the yield strength of Steel material). The randomness is generally modeled using random variables. On the other hand, the epistemic uncertainties originate from the incompleteness of data. This source of uncertainty is resulted from an incomplete modeling, simplification in the simulation, and limited access to the visualized actual behavior. The epistemic uncertainty includes the modeling,

as well as the statistical uncertainties. The modeling uncertainties can be resulted by the existing difference(s) between the actual structural behavior and its simplified form in the created mathematical models (such as finite element models). Statistical uncertainties are caused by the limited number of the samples available for presenting the statistical models. For instance, the probability distributions that express a random variable will represent the randomness of the given parameter. On the other hand, the errors in the prediction of the mean and standard deviation of the assumed probability distribution reflect the epistemic uncertainties of the problem [3].

To achieve a more accurate seismic design solution, the philosophy of performance-based earthquake engineering was introduced [1]. This approach relies on the more accurate understanding of the earthquake phenomenon seismologically, the increase in the computational power of computers, and the development of more accurate computational models to calculate the nonlinear dynamic response of structures. Within this philosophy, it is allowed to impose a certain degree of damage on the structures, while saving people during intensive earthquakes with the structure being remained intact against low and moderate earthquakes. Consequently, the corresponding structural performance is expected to be fulfilled against different levels of seismic hazard(s). According to the developed performance-based seismic design codes, the structural members are classified into the 'force-controlled' and 'deformation-controlled' groups according to their ability of tolerating the inelastic deformations (i.e., ductility). In both categories, however, the engineering parameters such as exerted forces and earthquake-induced deformations are the indicators of the seismic performance of the structures. The occurrence of large-scale earthquakes at the end of the twentieth century (such as the earthquakes of Loma Prieta in 1989, Northridge 1994, and Kobe in 1996) fulfilled the target of protecting people's lives (which was the goal of performance-based earthquake engineering) but caused substantial economic impacts and losses. Hence, the engineering community looked for a method to describe and control the seismic performance of structures by more inclusive variables, which are understandable by all stakeholders [4]. Furthermore, the lack of direct involvement of different sources of uncertainty in the seismic design of structures was one of the defects existed in the first generation of performance-based seismic design codes and standards. A method was recently proposed by the Pacific Earthquake Engineering Research Center (*PEER*) as part of the attempts towards developing the next generation of performance-based seismic design codes.

The effects of including uncertainties on the final seismic loss calculations, using the *PEER* method, were not investigated in the previous studies. Therefore, the overarching goal of the present study was to determine the effects of the modeling uncertainties on the final seismic loss curves of structures with buckling-restrained brace frames. To this end, 4-, 8-, and 12-story sample structures with buckling-restrained braces were designed in accordance with the appropriate codes. Subsequently, a sample frame, selected from the 3D structure, was modeled in the '*OpenSees*' finite element software using the *'Steel4'* material model. The finite element model was validated within the second phase of this study through the comparison of the finite element results with those of the experimental studies. Following the validation of the finite element model, the modulus of elasticity and yield stress of materials were selected as the modeling parameters that are affected by modeling uncertainties. The modeling uncertainties were incorporated into the final results using the first-order second-moment method (*FOSM*). Finally, the probabilistic curves of the seismic responses of the sample structures, the probability curves of the damage inflicted on the sample structures, and the probability curves of the final loss of the study frames were presented in two stages: 1) with the effects of the uncertainties mentioned above and, 2) without those effects.

2. *PEER* probabilistic method

In this section, the *PEER* probabilistic method is presented to calculate the seismic-induced risk to the structures. Using this method, the uncertain parameters, which affect the seismic performance of structures, include the earthquake intensity, structural response, structural damage, and structural loss. The relevant probability curves are used to express the uncertainties by each of the parameters as mentioned earlier. The probabilistic loss curve shows the infliction probability of a certain level of losses. Several studies have been conducted to determine the contributed probability distributions. Examples are of the studies already carried out in order to determine the seismic hazard models [5], the structural response probability models, and the structural fragility and loss curves for different structures [6-10]. Eventually, the seismic performance of the assumed structure is expressed by the calculated loss curve which is the combination of the probability distributions, as mentioned earlier, using the conditional probability theorem. This framework was introduced by Krawinkler and Cornell [11], and was developed by other researchers later on [12-15]. Figure (1) presents the framework for this method.

There are different methods such as Monte Carlo, which is a simple method with high computational costs, to include the effect of uncertainties on the response. However, the *FOSM* method has the capability of involving the effect of uncertainties at a lower computational cost [16]. Besides, the simple SRSS (square root of sum of squares) method is used

in some limit states to combine the inherent and epistemic uncertainties [17].

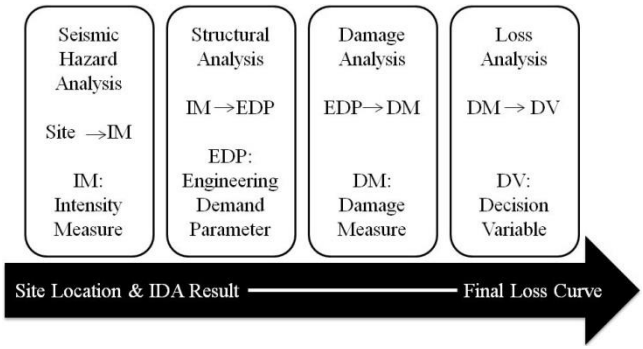

Fig. 1: The four probabilistic steps of seismic loss calculation for analysis of structures

These probabilities are integrated by using the total probability theorem presented by the below equation [18].

$$P(DV) = \iiint P[DV|DM]p[DM|EDP]p[EDP|IM]p[IM]dDMdEDPdIM \quad (1)$$

Where *DV* represents the decision variable, *DM* denotes the damage magnitude, *EDP* represents the engineering demand parameter, and *IM* denotes the earthquake intensity measure.

Extensive research was conducted on the effect of inherent and epistemic uncertainties on the seismic response of the structures. The effects of epistemic uncertainties such as the uncertainties associated with the material model and damping level [19, 20], geometry- and model-related parameters [21, 22], strength, stiffness, and capacity of structural members [23], and ductility capacity and cyclic failure were studied on the responses of steel moment-resisting frames [24, 25], concrete moment-resisting frames [26], steel braced frames, and buckling-restrained braced frames [27, 28]. In these studies, the inherent uncertainties resulting from earthquake records were taken into account by determining the structural response to a group of earthquake records. Moreover, the effect of uncertainties on the fragility curves in different limit states was investigated in the previous studies. These studies reflected the necessity of taking the various sources of uncertainties into account in each step of the analysis of the seismic performance of structures. However, the effect of epistemic uncertainties on the final seismic loss curve was not studied in the previous studies. The innovation of the present study is quantifying the impact of the epistemic uncertainties on the calculated seismic loss curves for the assumed structures. To study this effect, the buckling-restrained braced frames were selected as case studies.

The buckling-restrained brace system allows yielding under tension and compression actions without brace buckling and deterioration phenomena. Hence, it has a more stable hysteresis curve, and more energy dissipation capacity is reached due to its particular assembly procedure. A buckling-restrained brace is composed of a yielding metal core confined with a concrete shell. The concrete shell functions as a lateral support for the brace, preventing the metal core from buckling under the effect of the compressive forces. Consequently, the compressive strength of the member can rise to the yielding level without buckling, resulting in a more stable and symmetric behavior of the brace hysteresis curve. This outcome is highly satisfactory from the earthquake engineering point of view. From the numerical and experimental viewpoints, the first studies on the behavior of buckling-restrained frames were conducted by Wakabayashi et al. in Japan [29]. In 2013, Zsarnóczay carried out an experimental study on the buckling-restrained brace samples and developed a material model of the buckling-restrained braces as *'OpenSees'*, which was called the *Steel4* material model [28]. Besides, Zsarnóczay explored the effect of the modeling uncertainties on the seismic response and seismic fragility of the structures with buckling-restrained braces. In the abovementioned studies, the effects of uncertainties on the seismic response of the structures and the seismic damage probability curves were analyzed.

3. Sample structures

3.1 Modeling Assumptions

To study the effects of modeling uncertainties on the seismic-induced losses, three sample structures were considered. Numbers of stories were 4, 8, and 12, which were representatives for low, moderate, and high-rise structures, respectively. The lateral-resisting system was considered as BRB. The structural site was assumed as the high-risk category (i.e., subject to the seismic design acceleration of 0.35g) with soil type III based on Iranian national seismic code (standard No. 2800) classification. The yield strength and the modulus of elasticity of the steel material were 240MPa and 21GPa, respectively. The free distance between the columns (i.e., the bay width in the numerical model) and the story height of the sample structures were assumed to be 5 and 3 meters, respectively. The dead load and the live load of the roof were 500 and 150 kg/m^2, respectively; and the ones for the other stories were 590 and 300 kg/m^2, respectively; given the building as a commercial one. The seismic loading was carried out according to the Iranian National Seismic Code (Fourth edition of standard No. 2800) [30]. With the abovementioned assumptions, the three sample structures were analyzed three-dimensionally using ETABS. To achieve the structural performance using the *PEER* method, a sample frame was selected from 3D structures and modeled using *'OpenSees'*.

The typical plan of the sampled structures and the extracted frame are presented in Figure (2) and Figure (3), respectively.

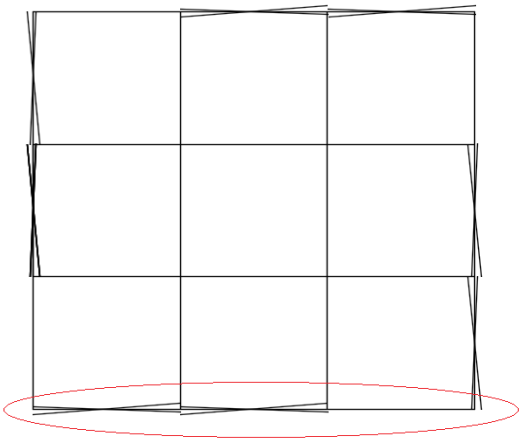

Fig. 2: The structure plan and the positions of the sample braces and frames

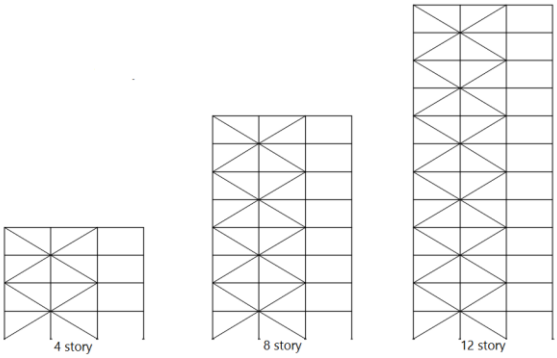

Fig. 3: BRB sample frames

The designed structural sections are presented in Table (1).

Table 1: The beam, column, and BRBF sections

Story	Column	Beam	BRB (mm^2)
4-story			
story1	Box 150 ×150 ×8	IPE240	25.80
story2-story3	Box 150 ×150 ×8	IPE240	12.90
story4	Box 150 ×150 ×8	IPE240	6.450
8-story			
story1-story2	Box 300×300 ×12	IPE 240	25.80
story3-story4	Box 240×240 ×8	IPE 240	22.58
story5	Box 240×240 ×8	IPE 240	22.58
story6-story7	Box 150×150 ×8	IPE 240	12.90
story8	Box 150×150 ×8	IPE 240	6.450
12-story			
story1	Box 350× 350 ×20	IPE 240	25.80
story2-story4	Box 300× 300×15	IPE 240	25.80
story5	Box 240× 240 ×12	IPE 240	22.58
story6	Box 240× 240 ×12	IPE 240	22.58
story7-story8	Box 240× 240 ×8	IPE 240	22.58
story9	Box 150 ×150 ×8	IPE 240	22.58
story10-story11	Box 150 ×150 ×8	IPE 240	12.90
story12	Box 150 ×150 ×8	IPE 240	6.450

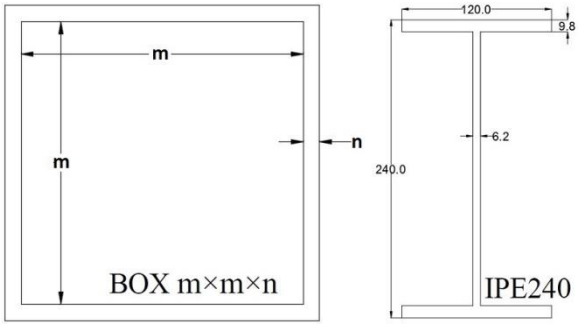

Fig. 4: BOX and IPE sections

Three frames are selected randomly from each of the three structures designed by ETABS and modeled two-dimensionally by 'OpenSees'.

3.2 Modeling assumptions using OpenSees

Since the structural lateral-resisting system was braced frames, the beam-to-column connections were pinned. Moreover, the fiber sections were used to model the beams and columns. To model the buckling-restrained braces *CorotTruss* element was used. *CorotTruss* element only transfers the axial force without buckling. As mentioned earlier, the *Steel02 'OpenSees'* material model was used to model the beams and columns, while the Steel4 material was used to model the braces. *Steel02* and Steel4 uniaxial material models mimic the *Giuffre-Menegotto-Pinto* hysteretic behavior [31] with isotropic hardening and combined kinetic, and isotropic hardening, respectively. Kinematic hardening was based on the *Menegotto-Pinto* model. The parameters and their usage in '*Steel04'* material model were identical to those in '*Steel02'* material model. Isotropic hardening increased the yield strength of the material and the increase magnitude was calculated as a function of the accumulated plastic strain.

The effect of fatigue on the materials was also taken into account. Since the structures were symmetric, the two-dimensional frames, which had responses similar to the three-dimensional structures, were used to reduce the computational cost. The effective mass of the structures was the combination of the dead load plus 0.6 times the live load [32].

3.3 Validation of OpenSees model using experimental results

To ensure the validity of the numerical model, it was essential to compare the numerical results with the relative experimental results. To do this, the tests implemented by Zsarnóczay [28], the C500w-1 buckling-restrained brace test under the C2 cyclic loading protocol, presented in Figure (5), were used. The total brace length of C500w-1 test was 2960mm, the yielding zone length was 2000mm, and the buckling-restrained cross section was 20 mm × 25 mm [28].

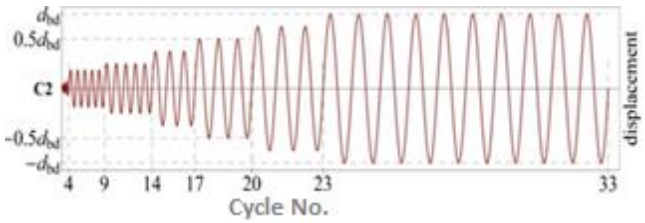

Fig. 5: The Loading of the experimental sample [28]

The mentioned test was modeled by OpenSees with boundary conditions under the cyclic loading protocol. The experimental and calculated hysteretic curves, are shown in Figures (6) and (7), respectively. As the figures show, there is an acceptable agreement between experimental and numerical hysteretic curves, which demonstrates the validity of the Steel4 model to simulate the BRB braces.

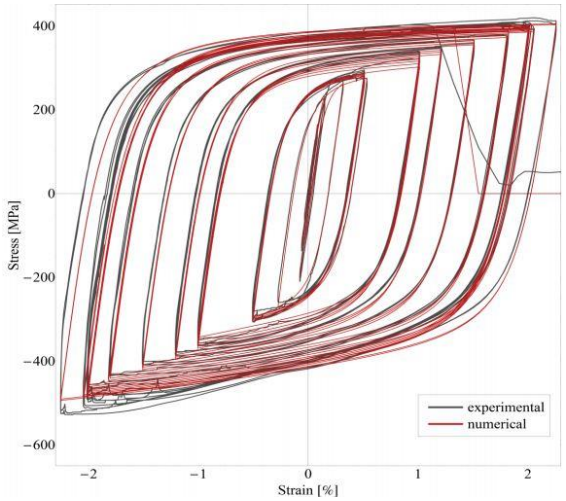

Fig. 6: The hysteresis curve of the C500W-1 sample by Zsarnóczay [28]

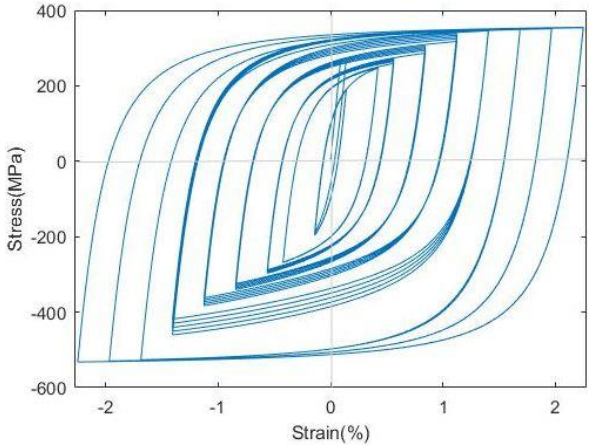

Fig. 7: The hysteresis curve of the C500W-1 sample resulted from modeling

Furthermore, the period of each of these three frames, modeled by OpenSees, was compared with those achieved using ETABS. The results of this comparison are listed in Table (2).

Table 2: The periods of different frames (seconds)

BRBF	OPENSEES	ETABS
4story	T_1=0.5179 T_2=0.2009	T_1=0.522 T_2=0.201
8story	T_1=0.889 T_2=0.329	T_1=0.897 T_2=0.325
12story	T_1=1.369 T_2=0.468	T_1=1.352 T_2=0.466

4. Sources of the Uncertainties

In the present study, the variability of the modulus of elasticity and the yield stress of the steel brace core form the source of uncertainties. The variation of these parameters has probability distributions, which was presented in the study by Kala et al. [22]. Table (3) shows the median and the standard deviation values of these parameters. To involve the effects of the mentioned uncertainties of the modeling parameters in the seismic-induced risk of the sample frames, the First Order Second Method (FOSM) was applied. Through this method, the relationships (presented by Equation (2)) are used to determine the mean and standard deviation values. If the hypothetical function g is dependent on the uncertain parameters (X_i), the mean value of g is calculated using the mean values of X_i. The standard deviation of g is calculated based on the first Taylor expansion of g, as below

$$\begin{aligned} Y &= g\left(X_1, X_2, ..., X_n\right) \\ \mu_Y &= g\left(\mu_{X_1}, \mu_{X_2}, ..., \mu_{X_n}\right) \\ \sigma_Y^2 &= \sum_{i=1}^{n}\sum_{j=1}^{n} \frac{\partial g}{\partial X_i}\frac{\partial g}{\partial X_j}\rho_{X_i X_j}\sigma_{X_i}\sigma_{X_j} \end{aligned} \quad (2)$$

In the equations above, μ_{xi} and σ_{xi} are the mean and standard deviation of X_i, respectively and ρ_{xixj} is the correlation coefficient of X_i and X_j . The derivative of the function g with respect to X_i is calculated based on Equation (3).

$$\frac{\partial g}{\partial X_i} = \frac{g\left(\mu_{x_i} + \sigma_{x_i}\right) - g\left(\mu_{x_i} - \sigma_{x_i}\right)}{2\sigma_{x_i}} \quad (3)$$

To implement the FOSM method, the values of function *g* for several values of X_i must be calculated.

In the present study, the values listed in Table (4) (which show the probabilities of 16%, 50%, and 84%) were used to involve the effects of uncertainties in the seismic performance of the sample structures, using *FOSM* method. Totally, nine simulations of the structures were created (three simulations for each parameter that is affected by uncertainties). Time-history analysis of the simulations against a set of strong ground motions presented the variability of the structural response due to the strong ground motion variability. The mean values of the structural response were achieved while the mean values of the modeling parameters (i.e., the value with 50% probability)

were chosen. The standard deviation of the structural responses was also calculated using the first two terms of the Taylor series (presented by Equation (2)). Besides, the effects of uncertainty of the modeling parameters on seismic-induced loss to the assumed structure were investigated similarly. To this end, the mean value of the loss curve was achieved based on the simulation with the mean values of the modeling parameters. The standard deviation values of seismic-induced losses were calculated based on Equation (2), for which the expected annual loss (*EAL*) was considered as *g* function. Therefore, the *EAL* of the simulated structures had to be calculated. To accomplish this goal using *PEER* methodology, probabilistic seismic hazard model, probabilistic seismic-induced structural response, probabilistic damage, and probabilistic loss model had to be specified.

Presenting the probabilistic seismic structural response model (or probabilistic seismic demand model (*PSDM)*) was the first step to calculate *EAL* for the simulated structures. The *PSDMs* for the simulated frames were achieved based on Incremental Dynamic Analysis (*IDA*). The *IDA* procedure and its application in view of attaining *PSDM* and seismic fragility curves are presented in the next section.

Table 3: The mean and standard deviation of the yield stress and the modulus of elasticity

Parameter	Density	Mean value	Standard deviation
Fy	Normal	267.2Mpa	15.1Mpa
E	Normal	210Gpa	12.6Gpa

Table 4: The different values of yield stress and modulus of elasticity

Probability	16%	50%	84%
Fy (Mpa)	252.1	267.2	282.3
E (Gpa)	197.4	210	222.6

5. Incremental Dynamic Analysis (*IDA*)

Incremental Dynamic Analysis (*IDA*) is the most comprehensive method towards calculating the structural response variability due to the randomness of the strong ground motions caused by earthquake. As the first step of this method, a set of strong ground motions weas selected. The selected strong ground motions should be compatible with the seismological and geological characteristics of the structural location, as the first criterion. On the other hand, the effects, which make the unwanted bias in the results should be avoided. For instance, strong ground motions containing near-fault effects (such as directivity and fling effects) insert an undesirable bias in the probabilistic model of the structural response values. Therefore, the motions containing these effects were not selected in the present study.

As the second criterion, the chosen strong ground motions should cover the expected magnitude and distance intervals. Regarding the required number of the strong ground motions to achieve the sufficiently confident response, the more the number of the records is, the more confidence and accuracy of the produced probabilistic demand model will be achieved. On the other hand, increasing the number of strong ground motions will drastically increase the required computational effort. As the second step of IDA, the selected strong ground motions were scaled at incrementally increased intensity levels. Plotting the structural response parameter versus the scaled intensity levels presents the overall structural behavior from elastic to yielding and dynamic instability. When the *IDA* curves were plotted for a number of strong ground motions and/or vibrations, the parameters of the probability distribution for the structural response at each *IM* level could be calculated based on fitting the probability function to the calculated response values. Required number of strong ground motions and the scaling methodology are still open fields of research, which were not investigated through the present study. Therefore, the spectral acceleration corresponding to the first-mode period (*SA* (T_1)) was selected as the *IM* parameter, and the maximum inter-story drift ratio was considered as the engineering demand parameter (*EDP*).

Medina et al. [33] gathered a record set, entitled *LMSR-N*[1], which included 40 earthquake records. In the present study, the same strong ground motions were used towards achieving the *PSDM*. The acceleration response spectra of the records are presented in Figure (8).

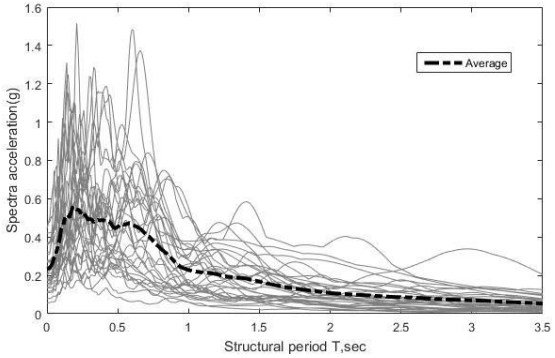

Fig. 8: The acceleration response spectra of the selected records

In order to have a more understandable presentation of *IDA* curves, they were summarized based on the percentiles of 16%, 50%, and 84% values using statistical methods. This approach was used to compare the *IDA* curves for the sample frames and various values of the modeling parameters. Figures (9) to (11) present the summarized curves, which

[1] New set of Large Magnitude with Short Distance records

were used through the FOSM method to involve the effects of modeling uncertainties on the final loss curves.

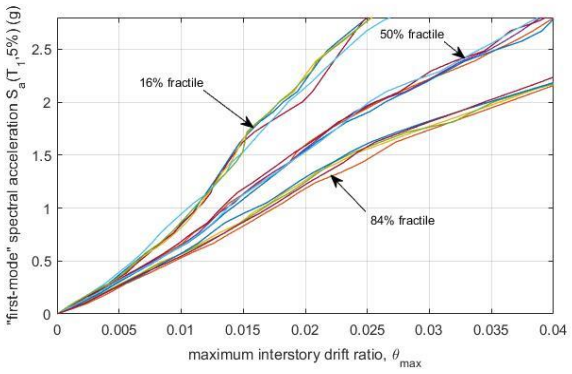

Fig. 9: IDA curves for the 4-story frame

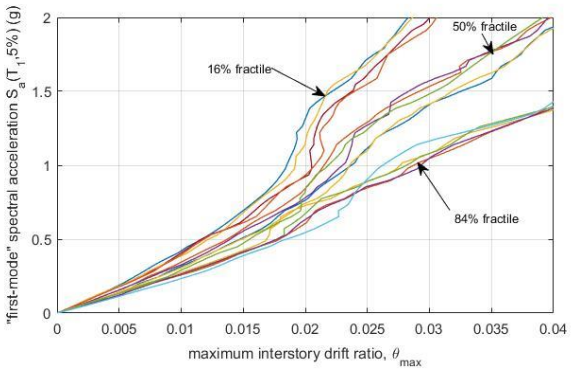

Fig. 10: IDA curves for the 8-story frame

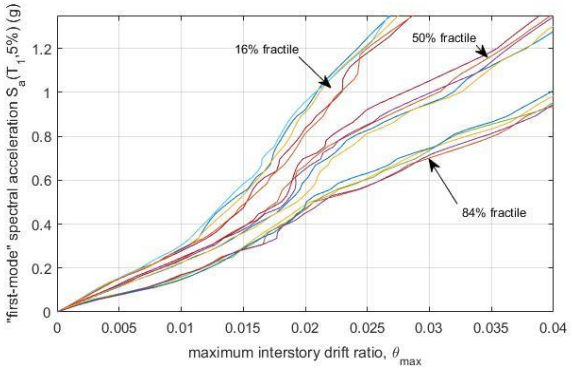

Fig. 11: IDA curves for the 12-story frame

6. Loss Analysis

To achieve the seismic-induced losses to the sample frames, *PEER* probabilistic framework was applied. The first step was the probabilistic seismic hazard analysis. PSHA shows the mean annual frequency of the exceedance for the selected strong ground motion intensity parameter (i.e., $SA(T_1)$). Cornel et al. [34] proposed the power function as the mathematical formulation of the *MAFE*, presented by Equation (4) as below.

$$\lambda(SA) = k_0 (SA)^{-k} \tag{4}$$

In which, λ and *SA* stand for the *MAFE* and spectral acceleration of the first-mode period, respectively; *K* and K_0 are constants that are calculated based on curve fitting to the calculated seismic hazard values for the assumed site. The uniform hazard spectra for the assumed structural location (i.e., 35.71 latitude and 51.31 longitude) are presented in Figure (12) for 475 and 2475 return periods [35]. Using the UHS for two hazard levels, the constants of the hazard function were calculated according to the nonlinear interpolation method.

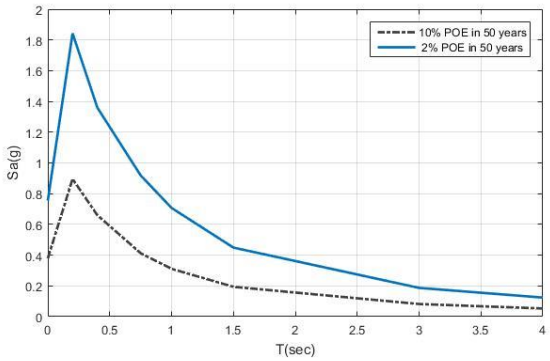

Fig. 12: The Uniform Hazard Spectra for 475 and 2475 return periods [35]

$$P(IM) = 1 - e^{-\lambda(IM)t} \tag{5}$$

$$p(IM) = -\frac{dp(IM)}{dIM} \tag{6}$$

Probabilistic seismic-induced structural demand analysis is the second step towards calculating the seismic loss. In order to involve modeling uncertainty effects on the seismic-induced losses using the *FOSM* method, the *IDA* analysis was conducted. Based on the achieved *IDA* curves (shown in the previous section), the probability distributions of *EDP* for various levels of IM were calculated. For brevity, samples of the *EDP* probability distributions are illustrated in Figures (13) to (15). The probability distributions are presented for two cases involving the effects of modeling uncertainties using the *FOSM* method and neglecting the modeling uncertainties (i.e., the modeling parameters are set to their mean values).

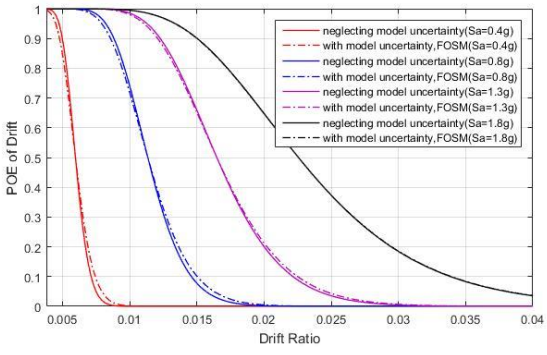

Fig. 13: The exceedance probability of MIDR for the 4-story frame

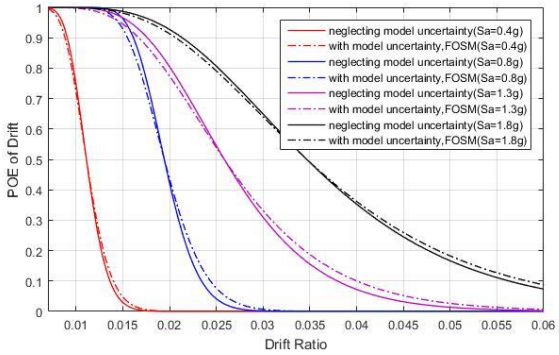

Fig. 14: The exceedance probability of MIDR for the 8-story frame

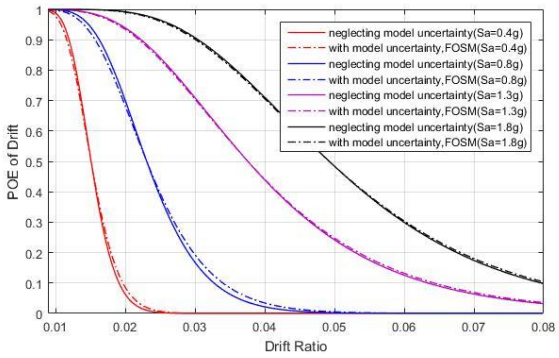

Fig. 15: The exceedance probability of MIDR for the 12-story frame

According to the calculated *EDP* probability distributions, the effect of the modeling uncertainties, caused by the yield stress and the modulus of elasticity, was more significant at lower intensities than the effects at higher levels of *IM*.

The third step of calculating the seismic-induced losses was the fragility analysis of the sampled frame. Through this step, the probabilistic amount of seismic-induced damages (*DM*) was presented conditioned on the imposed structural demand levels (*EDP*). In this study, the slight, moderate, and extensive damage levels were adopted from *HAZUS* [36]. The mean values of relevant fragility curves, in terms of maximum inter-story drift ratio (*MIDR*), were listed in Table (5). The standard deviation of 0.4 was assumed for the fragility curves of the mentioned damage levels. Figure (16) shows the fragility curves for 4- and 8- story sample frames (as the moderate-height structures based on *HAZUS*) and Figure (17) presents the fragility curves for the 12-story sample frame (as the higher structure based on *HAZUS*).

Table 5: Mean values of MIDR for various damage limit states

Limit states	Slight	Moderate	Extensive	Complete
Moderate	0.0033	0.0058	0.0156	0.04
High	0.0025	0.0043	0.0117	0.03

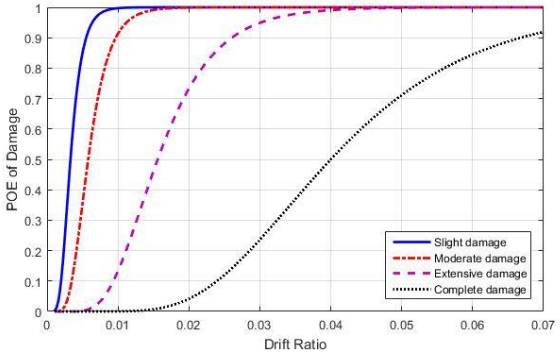

Fig. 16: The fragility curves of the slight, moderate, extensive, and complete damage states for the 4- and 8-story structures

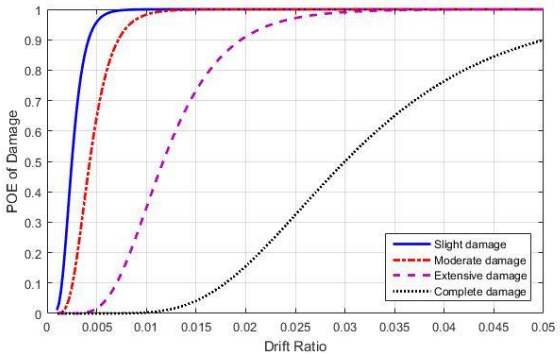

Fig. 17: The fragility curves of the slight, moderate, extensive, and complete damage states for the 12-story structure

The next step was presenting the probabilistic loss model conditioned on the seismic-induced damage levels. This step aimed to give the probability of exceedance of structural losses for a certain level of seismic-induced damages. The level of conditional loss was expressed in terms of the percentage of the Building Replacement Cost (*BRC*). The mean values of losses for each damage level were 2%, 10%, 50%, and 100% of BRC for the slight, moderate, extensive, and complete damage levels, respectively [36]. The probability distribution of the conditional loss was normal, with the coefficient of variation (*COV*) equal to 0.2913 [37]. Figure (18) shows the probability of exceedance of the seismic-induced loss.

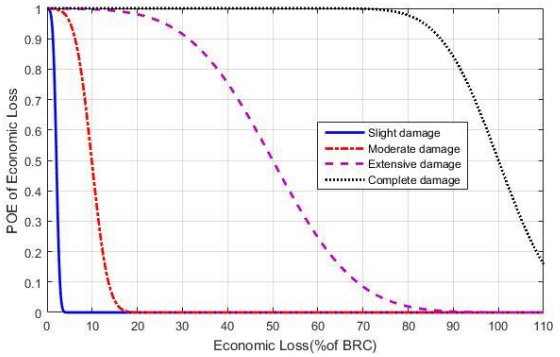

Fig. 18: The probability of exceedance of loss conditioned on the slight, moderate, extensive, and complete damage levels

Finally, the seismic loss curve, which shows the probability of exceedance of the economic loss, was obtained using the combination of all the previous steps by the *PEER* formulation. The achieved loss curves are depicted in Figures (19) to (21) for the three sample frames with and without involving the effects of modeling uncertainties.

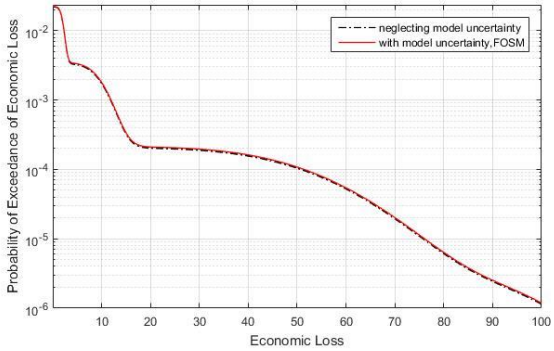

Fig. 19 : The final loss curve for the 4-story structure in terms of percentage of *BRC*

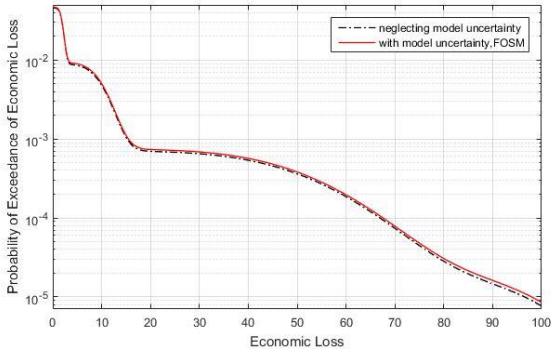

Fig. 20 : The final loss curve for the 8-story structure in terms of percentage of *BRC*

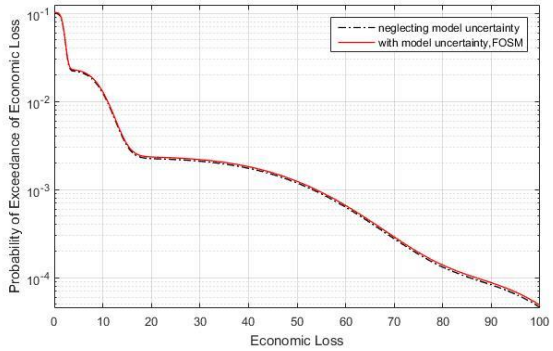

Fig. 21 : The final loss curve for the 12-story structure in terms of percentage of *BRC*

Table (6) shows the expected annual cost, which is the integration of the loss curve, in terms of the percentage of building replacement cost.

Table 6: Comparison of the expected annual costs (%BRC)

type	FOSM	Mean Parameters
4-story	0.080429	0.079796
8-story	0.198272	0.191133
12-story	0.490004	0.465826

The expected losses within 50 years for the 4-, 8-, and 12-story frames, considering two cases of neglecting modeling uncertainty effects (i.e., models with the mean values of the modeling parameters) and involving modeling uncertainty effects using the *FOSM*, are shown in Figures (22) to (24). To convert the expected annual costs of structures to expected losses in 50 years, the Equation (7) was used [38].

$$EL_{t-years} = EAL \times \left(\frac{1-e^{-it}}{i} \right) \quad (7)$$

In which EAL stands for expected annual loss, and *i* presents the annual discount rate. To calculate the loss values, the building replacement cost was estimated based on the weights of structures assuming the price of 10$ per kilogram of steel.

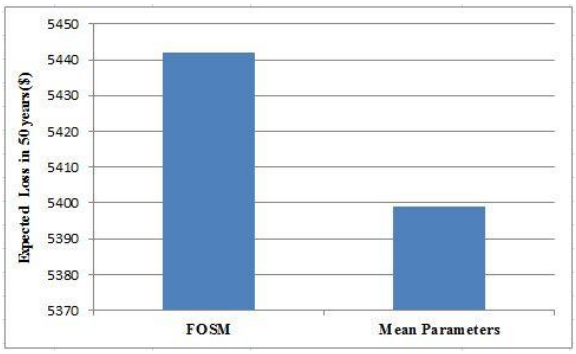

Fig. 22 : The expected loss within 50 years in the 4-story structure

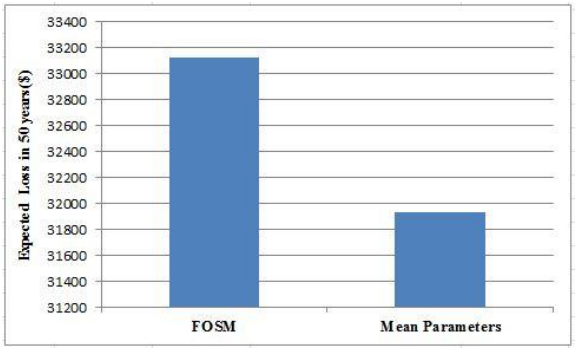

Fig. 23 : The expected loss within 50 years in the 8-story structure

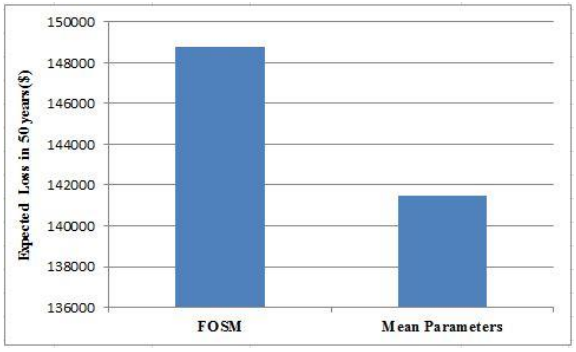

Fig. 24 : The expected loss within 50 years in the 12-story structure

7. Conclusion

In this study, the seismic-induced risk, in terms of economic losses of structural elements, was calculated based on the *PEER* probabilistic formulation for the sampled *BRB* frames. The financial losses were estimated considering the effects of uncertainties initiated from the variability of the modeling parameters and compared with those calculated neglecting the uncertainty effects. The modulus of elasticity and the yield stress of the steel material were the modeling parameters. The uncertainty effects were involved using the *FOSM* method. Probabilistic seismic hazard analysis based on the power formulation, probabilistic structural demand analysis based on the Incremental Dynamic Analysis of the sampled frames, probabilistic structural damage analysis and probabilistic consequence functions based on predefined fragility curves and loss functions by *HAZUS* were combined to achieve the *MAFE* curves of seismic-induced losses. Furthermore, the *EAL* values calculated based on the integration of *MAFE* curves were estimated in terms of the building replacement cost (*BRC*).

As shown in Figures (13) to (15), the effects of the existed uncertainty in yield stress and modulus of elasticity on the probability distributions of structural demand were more notable for the lower ground motion intensities. On the other hand, the structural demand probability distributions, for the higher levels of strong ground motions, were affected less by the mentioned uncertainties. This conclusion can be justified based on the fact that the structural response, against the higher levels of strong ground motion intensities, were profoundly affected by the modeling parameters beyond the elastic limits of the materials.

As illustrated in Figures (22) to (24), when the modeling uncertainties were involved, the expected losses of the sample frames in 50 years were increased by 0.8%, 3.8% and 5.7% for the 4-, 8- and 12-story sample frames, respectively. The results suggested that the predicted structural losses in the presence of these parameters were larger than the loss calculated neglecting these uncertainties. This result showed the necessity to involve the effects of various modeling uncertainty effects, while the performance of structures had to be calculated based on seismic-induced losses. Regarding the limitations of this study, it is worth mentioning that the losses to the structural elements were estimated while other contributors of seismic-induced losses, i.e., non-structural and content losses, were neglected. Furthermore, the fragility curves were considered based on the predefined *HAZUS* limit states. As an alternative, the fragility curves can be calculated based on *IDA* results. Calculations of fragility curves based on *IDA* results allows one to involve the uncertainty effects not only on the probabilistic seismic demand model but also on probabilistic structural damages. Moreover, the other methodologies such as response surface and Monte-Carlo methods are suggested to involve the effects of modeling uncertainties in seismic-induced losses.

References

[1] Hamburger, R.O. The ATC-58 project: development of next-generation performance-based earthquake engineering design criteria for buildings. in Structures Congress 2006: Structural Engineering and Public Safety. 2006.

[2] Yang, T., et al., Seismic performance evaluation of facilities: methodology and implementation. Journal of Structural Engineering, 2009. 135(10): p. 1146-1154.

[3] Zhang, H., R.L. Mullen, and R.L. Muhanna, Interval Monte Carlo methods for structural reliability. Structural Safety, 2010. 32(3): p. 183-190.

[4] Petak, W.J., and S. Elahi. The Northridge earthquake, USA and its economic and social impacts. in Euro-conference on global change and catastrophe risk management, earthquake risks in Europe, IIASA. 2000.

[5] Luco, N. and C.A. Cornell, Structure-specific scalar intensity measures for near-source and ordinary earthquake ground motions. Earthquake Spectra, 2007. 23(2): p. 357-392.

[6] Ibarra, L.F. and H. Krawinkler, Global collapse of frame structures under seismic excitations. 2005: Pacific Earthquake Engineering Research Center Berkeley, CA.

[7] Bradley, B.A. and D.S. Lee, Accuracy of approximate methods of uncertainty propagation in seismic loss estimation. Structural Safety, 2010. 32(1): p. 13-24.

[8] Baker, J.W. and C.A. Cornell, Uncertainty propagation in probabilistic seismic loss estimation. Structural Safety, 2008. 30(3): p. 236-252.

[9] Padgett, J.E. and R. DesRoches, Methodology for the development of analytical fragility curves for retrofitted bridges. Earthquake Engineering & Structural Dynamics, 2008. 37(8): p. 1157-1174.

[10] Shinozuka, M., et al., Statistical analysis of fragility curves. Journal of engineering mechanics, 2000. 126(12): p. 1224-1231.

[11] Cornell, C. and H. Krawinkler, Progress and challenges in seismic performance assessment. PEER Center News, Spring 2000. 2000.

[12] Porter, K.A. An overview of PEER's performance-based earthquake engineering methodology. in Proceedings of ninth international conference on applications of statistics and probability in civil engineering. 2003.

[13] Krawinkler, H. A general approach to seismic performance assessment. in Proceedings. 2002.

[14] Krawinkler, H. and E. Miranda, Performance-based earthquake engineering. 2004, CRC Press: Boca Raton, FL. p. 1-9.

[15] Moehle, J. and G.G. Deierlein. A framework methodology for performance-based earthquake engineering. in 13th world conference on earthquake engineering. 2004.

[16] Baker, J.W. and C.A. Cornell, Uncertainty specification and propagation for loss estimation using FOSM methods. 2003: Pacific Earthquake Engineering Research Center, College of Engineering.

[17] Vamvatsikos, D. and M. Fragiadakis, Incremental dynamic analysis for estimating seismic performance sensitivity and uncertainty. Earthquake engineering & structural dynamics, 2010. 39(2): p. 141-163.

[18] Deierlein, G.G. Overview of a comprehensive framework for earthquake performance assessment. in Performance-Based Seismic Design Concepts and Implementation, Proceedings of an International Workshop. 2004.

[19] Hardyniec, A. and F. Charney, An investigation into the effects of damping and nonlinear geometry models in earthquake engineering analysis. Earthquake Engineering & Structural Dynamics, 2015. 44(15): p. 2695-2715.

[20] Hajirasouliha, I., K. Pilakoutas, and R.K. Mohammadi, Effects of uncertainties on seismic behavior of optimum designed braced steel frames. Steel and Composite Structures, 2016. 20(2): p. 317-335.
[21] Kala, Z., Sensitivity assessment of steel members under compression. Engineering Structures, 2009. 31(6): p. 1344-1348.
[22] Kala, Z., J. Melcher, and L. Puklický, Material and geometrical characteristics of structural steels based on statistical analysis of metallurgical products. Journal of Civil Engineering and Management, 2009. 15(3): p. 299-307.
[23] Liel, A.B., et al., Incorporating modeling uncertainties in the assessment of seismic collapse risk of buildings. Structural Safety, 2009. 31(2): p. 197-211.
[24] Asgarian, B. and B. Ordoubadi, Effects of structural uncertainties on seismic performance of steel moment resisting frames. Journal of Constructional Steel Research, 2016. 120: p. 132-142.
[25] Kazantzi, A., D. Vamvatsikos, and D. Lignos, Seismic performance of a steel moment-resisting frame subject to strength and ductility uncertainty. Engineering Structures, 2014. 78: p. 69-77.
[26] Celik, O.C. and B.R. Ellingwood, Seismic fragilities for non-ductile reinforced concrete frames–Role of aleatoric and epistemic uncertainties. Structural Safety, 2010. 32(1): p. 1-12.
[27] Uriz, P. and S.A. Mahin. Seismic performance assessment of concentrically braced steel frames. in Proceedings of the 13th world conference on earthquake engineering. 2004.
[28] Zsarnóczay, Á., Experimental and numerical investigation of buckling restrained braced frames for Eurocode conform design procedure development. Budapest University of Technology and Economics, 2013.
[29] Wakabayashi, M., et al. Experimental study of elastoplastic properties of precast concrete wall panels with built-in insulating braces. in Summaries of Technical Papers of Annual Meeting. 1973. Architectural Institute of Japan.
[30] No, S., 2800 "Iranian Code of Practice for Seismic Resistant Design of Buildings." 4rd edition, PN S 253, Building and Housing Research Center, Tehran, 2015.
[31] Menegotto, M. and P. Pinto, Method of Analysis for Cyclically Loaded Reinforced Concrete Plane Frames Including Changes in Geometry and Non-elastic Behavior of Elements Under Combined Normal Force and Bending. Proceedings. IABSE Sympoium on Resistance and Ultimate Deformability of Structures Acted on by Well-Defined Repeated Loads, 1973.
[32] Richards, P.W., Seismic column demands in ductile braced frames. Journal of Structural Engineering, 2009. 135(1): p. 33-41.
[33] Medina, R.A. and H. Krawinkler, Seismic demands for nondeteriorating frame structures and their dependence on ground motions. 2004, Pacific Earthquake Engineering Research Center.
[34] Cornell, C.A., et al., Probabilistic basis for 2000 SAC federal emergency management agency steel moment frame guidelines. Journal of structural engineering, 2002. 128(4): p. 526-533.
[35] ; Available from: https://iranhazard.mporg.ir.
[36] HAZUS, M., MR4 Technical Manual. Multihazard Loss Estimation Methodology, 2003.
[37] FEMA, P., 58-3, Seismic Performance Assessment of Buildings, Volume 3–Supporting Electronic Materials and Background Documentation: 3.1 Performance Assessment Calculation Tool (PACT), Version 2.9. 65, Building seismic safety council for the Federal Emergency Management Agency, Report. Google Scholar, 2012.
[38] Porter, K.A., J.L. Beck, and R. Shaikhutdinov, Simplified estimation of economic seismic risk for buildings. Earthquake Spectra, 2004. 20(4): p. 1239-1263.

Appendix: Iranian Seismic Design Code

According to Iranian seismic code (Standard No. 2800), the structural seismic-induced base shear is calculated as a coefficient of the effective weight of structures.

$$V = CW \tag{A.1}$$

In which, the seismic coefficient C contains the effects of regional seismicity, soil type, structural occupancy and structural ductility. W is the effective weight of structure which is composed of dead load and a percentage of live load. The percentage is presented based on the building occupancy.

The seismic coefficient is calculated based on the following equation.

$$C = \frac{ABI}{R} \tag{A.2}$$

In which, A shows the earthquake design acceleration (acceleration level with the exceedance probability of 10% in 50 years). Based on Iranian seismic code, four seismic zones are defined, namely very high, high, moderate and low seismicity regions. The numerical values of A are 0.35, 0.3, 0.25 and 0.2 of gravitational acceleration.

B is the reflection factor, which aims to involve effects of soil type on seismic design force. Based on the fourth edition of Iranian seismic design code, the reflection factor is calculated according to the following equation:

$$B = \begin{cases} S_0 + (S - S_0 + 1)\left(\dfrac{T}{T_0}\right) & 0 < T < T_0 \\ S + 1 & T_0 < T < T_s \\ (S+1)\dfrac{T_s}{T} & T > T_s \end{cases} \tag{A.3}$$

In which, S, S_0, T_s, and T_0 are presented based on soil type and regional seismicity.

I is the importance factor, which depends on structural occupancy between 0.8 and 1.4, and R is the seismic force-reduction factor (behavior factor), which aims to involve effects of redundancy over strength and ductility of the assumed structure.